

A Guide to Design Disturbance Observer-based Motion Control Systems in Discrete-time Domain

Emre Sariyildiz

School of Mechanical, Materials, Mechatronic and Biomedical Engineering,
University of Wollongong, NSW, 2522, Australia.
emre@uow.edu.au

Abstract- This paper analyses and synthesises the Disturbance Observer (DOb) based motion control systems in the discrete-time domain. By employing Bode Integral Theorem, it is shown that continuous-time analysis methods fall-short in explaining the dynamic behaviours of the DOb-based robust motion controllers implemented by computers and microcontrollers. For example, continuous-time analysis methods cannot explain why the robust stability and performance of the digital motion controller deteriorate as the bandwidth of the DOb increases. Therefore, unexpected dynamic responses (e.g., poor stability and performance, and high-sensitivity to disturbances and noise) may be observed when the parameters of the digital robust motion controller are tuned by using continuous-time synthesis methods in practice. This paper also analytically derives the robust stability and performance constraints of the DOb-based motion controllers in the discrete-time domain. The proposed design constraints allow one to systematically synthesise a high-performance digital robust motion controller. The validity of the proposed analysis and synthesis methods are verified by simulations.

Index Terms: Discrete-time Control, Disturbance Observer, Motion Control, Robust Control, Robust Stability and Performance.

I. INTRODUCTION

It is a well-known fact that the stability and performance of a motion control system may significantly deteriorate by internal and external disturbances (e.g., friction, parametric uncertainties and unknown dynamics in plant model, and load) in real world applications [1–5]. To deal with this problem, various adaptive and robust motion control techniques, such as Sliding Mode Control, H_∞ control, Internal Model Control and Robust Parametric Control, have been proposed in the last decades [4–9]. Among them, the DOb is one of the most widely used robust motion control tools due to its simplicity and efficacy [1, 10].

The DOb-based robust motion controller synthesis is based on a simple and elegant idea: cancelling disturbances via feedforward control. The internal and external disturbances of a motion control system are cancelled by feedforwarding the reverse of the disturbance signal [1]. This intuitive robust motion controller design technique has attracted many control engineering practitioners, and the DOb has been applied to various engineering systems (e.g., robots, hard-disk drives, automobiles, satellites and unmanned aerial vehicles) in the last three decades [1, 11–15].

However, the feedforward robust controller synthesis is impractical because the internal and external disturbances are generally unknown in motion control systems [1]. In practice, the disturbances are estimated by using the measureable states and known plant dynamics, i.e., DOb, and the robust motion controller is synthesised by feedforwarding the reverse of the

estimated disturbance signal. In other words, a feedback robust motion controller is implicitly synthesised [1, 16, 17]. The stability and performance of the robust motion controller are directly influenced by the dynamics of disturbance estimation, i.e., the design parameters of the DOb [18]. For example, it is a well-known fact that the stability of the DOb-based robust motion controller deteriorates as the nominal inertia decreases [16, 17]. It is therefore very important to understand how the dynamic response of the robust motion controller changes by the design parameters of the DOb.

To improve the robust stability and performance of the DOb-based motion control systems, several analysis and synthesis methods have been proposed in the literature [16–20]. Although computers and microcontrollers are always employed in the implementation of the robust motion controllers, continuous-time analysis methods are generally used due to simplicity [1, 21]. However, continuous-time analysis methods cannot explain all dynamic responses, such as poor stability and performance, of the DOb-based robust motion controller implemented by computers and/or microcontrollers. For example, it is shown that the DOb-based digital robust motion control systems may exhibit under-damped and even unstable responses as the bandwidth of disturbance estimation increases in [22–24]. In section III, this paper clarifies why continuous-time analysis methods fall-short in explaining the dynamic behaviours of the DOb-based digital robust motion controllers by employing Bode Integral Theorem [25]. The following studies analyse and synthesise the DOb-based robust motion controllers in the discrete-time domain: bilinear transformation is used in [26, 27], sensitivity optimisation method is used to obtain better tracking performance than bilinear transformation in [28], disturbance suppression is improved by using multi-rate sampling control method in [29], optimal plant models are proposed to improve the bandwidth of disturbance estimation in [30, 31], Kalman filter is combined with the DOb to improve disturbance estimation in [32]. Nevertheless, the robust stability and performance of the DOb-based digital robust motion controllers have not been discussed in detail [24, 33]. Moreover, the design constraints of the DOb-based motion control systems have not yet been derived in the discrete-time domain.

This paper proposes a guide to design the DOb-based digital robust motion control systems. The design constraints of the digital robust motion controller (i.e., the bandwidth of the DOb, nominal plant model and sampling frequency) are analytically derived in discrete-time. The proposed design constraints allow one to systematically synthesise a high-performance robust digital motion controller. Bode Integral Theorem is employed in the continuous- and discrete- time

$$\int_0^{\infty} \log(|S_i(j\omega)|) d\omega = \pi \sum_k \operatorname{Re}(p_{u_k}^i) - \frac{\pi}{2} \lim_{s \rightarrow \infty} sL_i(s) = 0 \quad (4)$$

where ω is frequency, $j^2 = -1$ is complex number and $\operatorname{Re}(p_{u_k}^i)$ is the real part of the k^{th} right-half-plane pole of $L_i(s)$ [18, 25].

Since the right hand side of Eq. (3) gets a lower value as α and/or g_{DOB} are increased, the Bode's integral equation can hold without a high-sensitivity peak as the robustness and phase margin of the motion control system are improved. In other words, *waterbed effect* is not observed, and good robust stability and performance can be achieved for all values of the design parameters of α and g_{DOB} when the DOB is synthesised by using ideal velocity measurement, i.e., g_v is infinite. As the robustness against disturbances is improved by increasing either α or g_{DOB} , the peak of the sensitivity function increases to hold the Bode's integral equation given in Eq. (4). In other words, the robust motion controller may be subject to *waterbed effect* when a low-pass-filter is used in velocity measurement. This makes the robust motion control system more sensitive to disturbances at middle/high frequencies and degrades the robust stability and performance. However, the continuous-time analysis shows that the robust motion controller is stable for all values of the design parameters of α and g_{DOB} [35].

The reader is invited to refer to [17, 35] for further details on the robustness analysis of the DOB in the continuous-time domain. Although continuous-time analysis methods provide good understanding for the asymptotic dynamic behaviours of the digital robust motion controller (e.g., the robustness against disturbances improves at low frequencies as the bandwidth of the DOB increases), they fall-short in explaining some dynamic responses. For example, it is a well-known fact that the digital robust motion controller exhibits oscillatory response and becomes unstable as the phase margin and robustness of the DOB are increased although Eqs. (1) – (4) show that the robust motion controller is stable for all values of the design parameters of α and g_{DOB} [22–24]. Therefore, we may observe some unexpected dynamic responses when we analyse and synthesise the DOB-based digital robust motion controller in the continuous-time domain.

Let us now analyse the robust motion controller illustrated in Fig. 1b. The outer-loop's sensitivity and complementary sensitivity transfer functions are as follows:

$$S_o(s) = \frac{1}{1+L_o(s)} \quad \text{and} \quad T_o(s) = \frac{L_o(s)}{1+L_o(s)} \quad (5)$$

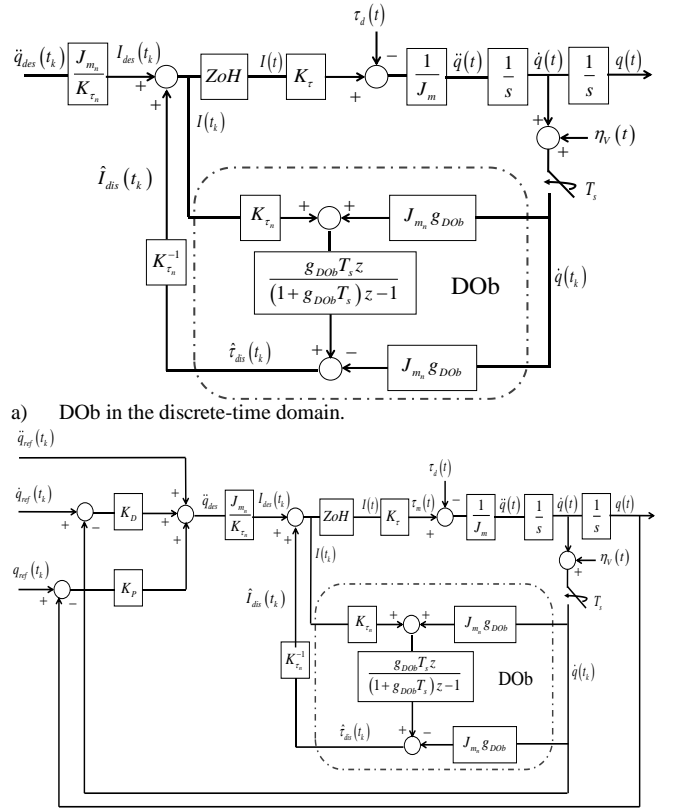
where $L_o(s) = \alpha \frac{g_{DOB}s^2 + (s + g_{DOB})(K_D s + K_P)}{s^3}$ when g_v is

infinite and $L_o(s) = \alpha \frac{g_v g_{DOB} s^2 + (s + g_v)(s + g_{DOB})(K_D s + K_P)}{s^3 (s + g_v)}$

when g_v is finite.

Equation (5) shows that the dynamics of the DOB directly influences the stability and performance of the robust motion controller. For example, the following design constraint should hold to achieve stability [17].

$$\alpha^{-1} < 1 + g_{DOB} \left(\frac{K_D}{K_p} + \frac{K_D}{g_{DOB}} + \frac{K_D^2}{K_p} \right) \quad (6)$$



b) DOB-based robust position controller in the discrete-time domain. Fig. 2: Block diagrams of the DOB and the robust motion controller in the discrete-time domain.

Equation (5) also shows that not only the DOB but also the outer-loop performance controller influences the robustness of the motion controller. As the control gains K_p and K_D are increased, the robustness against disturbances improves.

Although it is generally assumed that the robustness and performance of the DOB-based motion controllers can be independently adjusted in the inner- and outer- loop, respectively, Eq. (5) shows that this assumption is incorrect. The outer-loop controller can be used to tune the robustness, and the design parameters of the DOB can be used to tune the stability and performance of the motion controller [35]. In general, the bandwidth of the inner-loop is set higher than that of the outer-loop so that the influence of the disturbance estimation dynamics is suppressed [1, 17].

III. DOB-BASED ROBUST MOTION CONTROLLER IN THE DISCRETE-TIME DOMAIN

Block diagrams of the DOB and the robust motion controller are illustrated in the discrete-time domain in Fig. 2. In this figure, T_s represents sampling time, t and t_k represent time in the continuous- and discrete- domains, respectively, z represents a complex variable, and ZoH represents zero-order-hold. The other parameters are defined earlier.

The inner-loop transfer functions between the exogenous inputs and the acceleration can be derived from Fig. 2a as follows:

$$\ddot{q} = \alpha \frac{(1 + g_{DOB} T_s) z - 1}{z - (1 - \alpha g_{DOB} T_s)} \ddot{q}_{des} - \frac{1}{J_m} S_i(z) \tau_d - \frac{(z-1)}{T_s} T_i(z) \eta_v \quad (7)$$

where $S_i(z) = \frac{1}{1+L_i(z)} = \frac{z-1}{z-(1-\alpha g_{DOB} T_s)}$ and $T_i(z) = \frac{L_i(z)}{1+L_i(z)} = \frac{\alpha g_{DOB} T_s}{z-(1-\alpha g_{DOB} T_s)}$ are the inner-loop's sensitivity and

complementary sensitivity transfer functions in which

$$L_i(z) = \frac{\alpha g_{DOB} T_s}{z-1}.$$

Similar to the continuous-time analysis given in Eq. (1), Eq. (7) shows that a phase-lead (phase-lag) compensator is implicitly synthesised when the design parameters of the DOB are tuned by using $\alpha > 1/(1+g_{DOB}T_s)$ ($\alpha < 1/(1+g_{DOB}T_s)$). The phase-margin of the robust motion controller improves as α is increased. Since the sensitivity function gets smaller values at low frequency range, the robustness against disturbances can be improved by increasing either α or g_{DOB} . However, Eq. (7) shows that the inner-loop transfer functions become unstable when $\alpha g_{DOB}T_s > 2$, and the robust motion controller exhibits oscillatory response when $\alpha g_{DOB}T_s > 1$. In other words, neither α nor g_{DOB} can be freely increased to improve the phase-margin and the robustness of the motion controller.

Let us employ Bode Integral Theorem to analyse the robustness of the DOB in the discrete-time domain [25]. The Bode integral equation of the DOB illustrated in Fig. 2a is as follows:

$$\int_{-\pi}^{\pi} \ln |S_i(e^{j\omega T_s})| d\omega T_s = -2\pi \ln \left| 1 + \lim_{z \rightarrow \infty} L_i(z) \right| = 0 \quad (8)$$

To hold Eq. (8) within a limited frequency range (i.e., between $-\pi$ rad/s and π rad/s), the peak of the sensitivity function increases as the robustness of the motion controller improves by increasing either α or g_{DOB} . In other words, the DOB-based digital robust motion controller is subject to *waterbed effect* even ideal velocity measurement (g_v is infinite) is employed in the controller synthesis. As shown in section II, this dynamic behaviour of the digital robust motion controller cannot be deduced by conducting analysis in the continuous-time domain.

Let us consider the relation between the peaks of the sensitivity functions and the design parameters of the DOB in detail. The frequency responses of the inner-loop's sensitivity and complementary sensitivity transfer functions are as follows:

$$S_i(j\omega T_s) = \frac{\cos(\omega T_s) + j \sin(\omega T_s) - 1}{\cos(\omega T_s) + j \sin(\omega T_s) - (1 - \alpha g_{DOB} T_s)} \quad (9)$$

$$T_i(j\omega T_s) = \frac{\alpha g_{DOB} T_s}{\cos(\omega T_s) + j \sin(\omega T_s) - (1 - \alpha g_{DOB} T_s)} \quad (10)$$

When $2 > \alpha g_{DOB} T_s > 0$ (the stability constraint given in Eq. (7)), the maximum values of the sensitivity and complementary sensitivity functions appear at $\omega = T_s^{-1}(\pi + 2k\pi)$ rad/s as follows:

$$|S_i(j\omega T_s)|_{\max} = |S_i(j\pi)|_{\max} \frac{2}{|\alpha g_{DOB} T_s - 2|} \quad (11)$$

$$|T_i(j\omega T_s)|_{\max} = |T_i(j\pi)|_{\max} \frac{\alpha g_{DOB} T_s}{|\alpha g_{DOB} T_s - 2|} \quad (12)$$

If we assume that the sensitivity and complementary sensitivity functions satisfy $|S_i(j\omega T_s)|_{\max} \leq 1/\Gamma_{S_i}$ and $|T_i(j\omega T_s)|_{\max} \leq 1/\Gamma_{T_i}$, then the design constraints of the digital robust motion controller are derived as follows:

$$0 < \alpha g_{DOB} T_s \leq 2(1 - \Gamma_{S_i}) \quad (13)$$

$$0 < \alpha g_{DOB} T_s \leq 2/(1 + \Gamma_{T_i}) \quad (14)$$

where $0 < \Gamma_{S_i} < 1$ and $0 < \Gamma_{T_i} < 1$.

Let us now analyse the digital robust motion controller illustrated in Fig. 2b. For the sake of simplicity, the outer-loop performance controller is synthesised by using position measurement and Backward Euler method. The outer-loop transfer functions are derived from Fig. 2b as follows:

$$S_o(z) = \frac{1}{1 + L_o(z)} \quad \text{and} \quad T_o(s) = \frac{L_o(z)}{1 + L_o(z)} \quad (15)$$

where $L_o(z) = C(z)C_i(z)G_p(z)$ in which $C(z) = K_p + K_D \frac{z-1}{T_s z}$

$$C_i(z) = \alpha \frac{(1 + g_{DOB} T_s)z - 1}{z - (1 - \alpha g_{DOB} T_s)} \quad \text{and} \quad G_p(z) = \frac{T_s^2}{2} \frac{z+1}{(z-1)^2} \quad [22].$$

Equation (15) similarly shows that the design parameters of the DOB may significantly influence the stability and performance of the digital robust motion controller. For example, the stability can be improved by tuning $\alpha > 1/(1+g_{DOB}T_s)$, i.e., designing $C_i(z)$ as a phase-lead compensator. Besides, the robustness against disturbances can be improved by properly tuning the outer-loop performance controller so that lower values of the sensitivity function is obtained at low-frequencies.

IV. SIMULATION RESULTS

In this section, simulation results are given to verify the proposed analysis and synthesis methods.

Let us start with the continuous-time analysis methods. Figure 3 illustrates the frequency responses of the sensitivity and complementary sensitivity transfer functions when the nominal inertia and the bandwidth of the DOB are set at

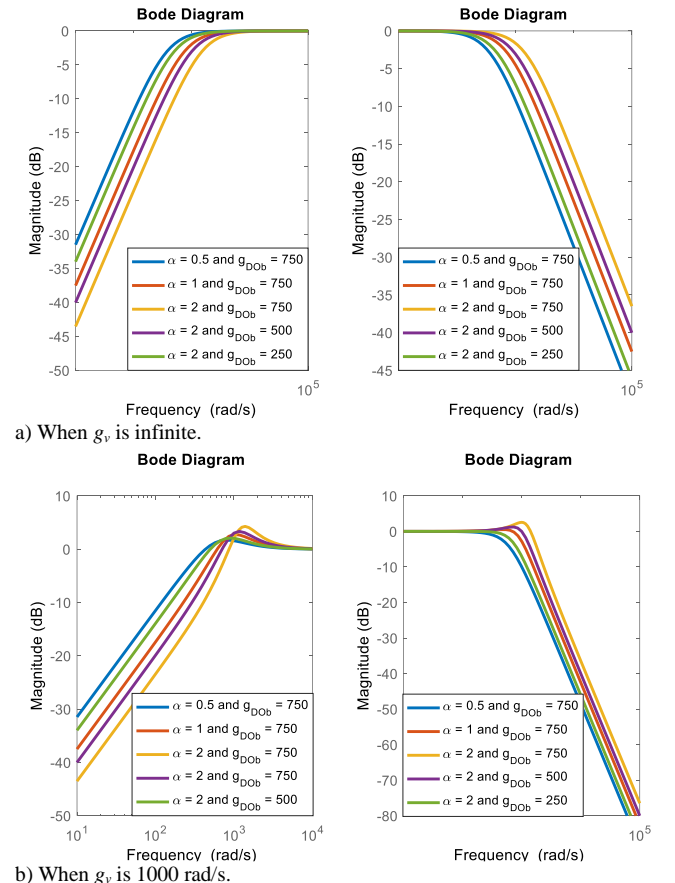
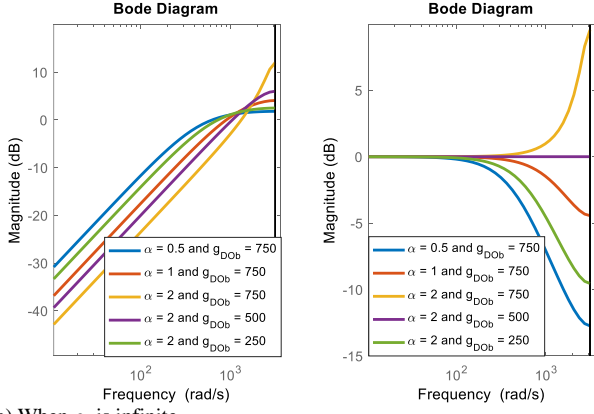
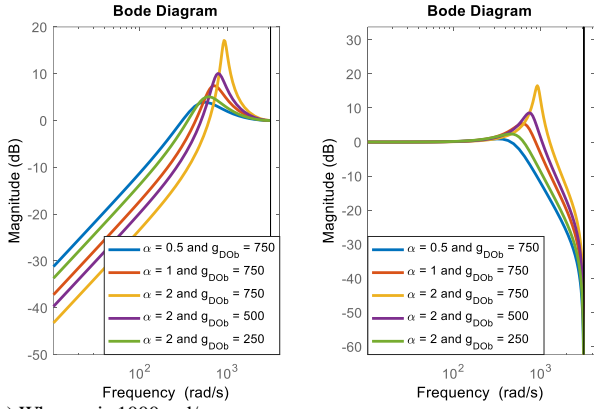


Fig.3. Sensitivity (left-figures) and complementary sensitivity (right-figures) functions' frequency responses in the continuous-time domain.



a) When g_v is infinite.

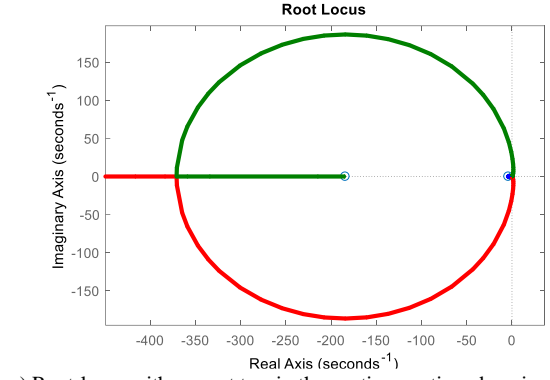


b) When g_v is 1000 rad/s.

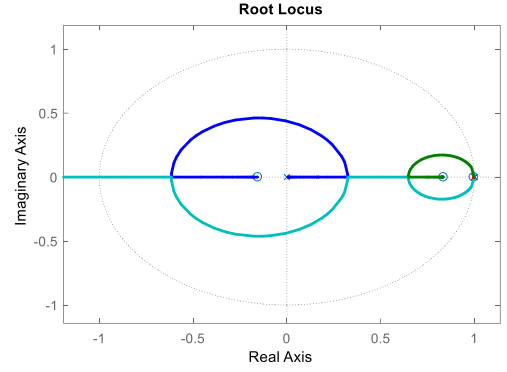
Fig. 4. Sensitivity (left-figures) and complementary sensitivity (right-figures) functions' frequency responses in the discrete-time domain when $T_s = 1$ ms. different values. It is clear from this figure that good robust stability and performance can be achieved for all values of the design parameters of α and g_{Dob} when ideal velocity measurement is employed in the DOB synthesis. However, the robust motion controller is subject to *waterbed effect* and the peak of the sensitivity and complementary sensitivity function increases as the robustness against disturbances is improved when g_v is finite.

Let us now analyse the DOB-based robust motion controller in the discrete-time domain. Figure 4 illustrates the frequency responses of the sensitivity and complementary sensitivity transfer functions for different values of α and g_{Dob} . As the robustness against disturbances is improved by increasing the bandwidth of the DOB or the phase margin is improved by increasing/decreasing the nominal inertia/thrust coefficient, the peaks of the sensitivity and complementary sensitivity transfer functions increase. This makes the robust motion controller more sensitive to disturbances at high frequencies such as noise and degrades the robust stability and performance.

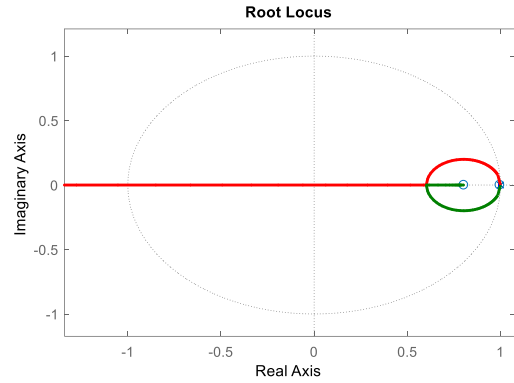
Let us now consider the stability of the robust motion controller. Figure 5 illustrates the root-loci of the motion control system with respect to α and g_{Dob} in the continuous- and discrete- time domains. This figure shows that the robust motion controller becomes unstable for small values of α and the stability is improved with phase-lead effect when α is increased. However, only the discrete-time analysis shows that the robust motion controller becomes unstable for high-values of α . Similarly, Fig. 5c shows that the digital robust motion controller becomes unstable as the bandwidth of the DOB is increased.



a) Root-locus with respect to α in the continuous-time domain.



b) Root-locus with respect to α in the discrete-time domain.



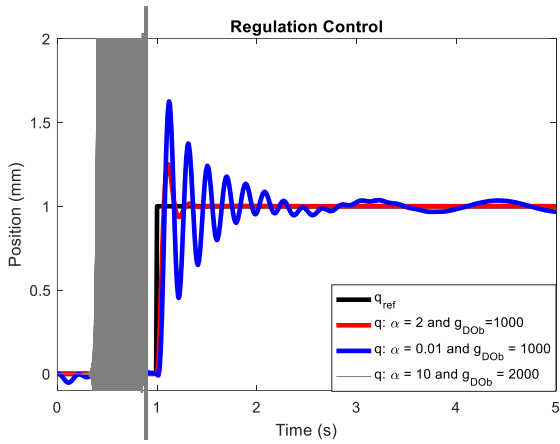
c) Root-locus with respect to g_{Dob} in the discrete-time domain. $\alpha = 0.01$.

Fig. 5. Root-loci of the robust motion controller. The parameters of the simulations are $J_m = 0.003$, $K_t = 0.25$, $g_{Dob} = 750$, $K_P = 1000$, $K_D = 250$, and $T_s = 1$ ms.

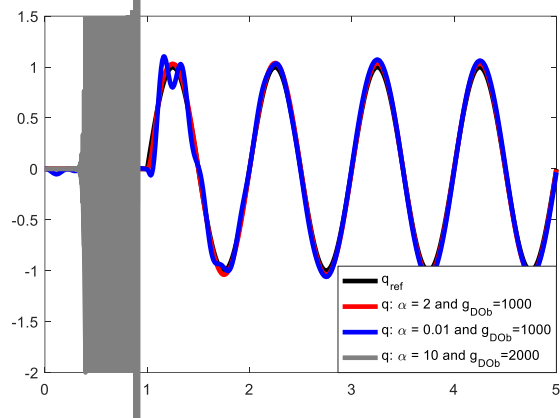
Last, let us present robust position control results. In this simulation, it is assumed that a servo system is affected by internal and external disturbances. Figure 6 shows that the robust position controller can precisely follow regulation and trajectory tracking control references by suppressing internal and external disturbances when it is synthesised by employing the design constraints derived in section III. When the design constraints are not satisfied (e.g., blue curves for $\alpha \ll 1$ and grey curves for $\alpha g_{Dob} T_s > 1$), oscillatory and unstable responses are observed.

V. CONCLUSION

In this paper, the stability and robustness of the DOB-based motion control systems are analysed in the continuous- and discrete- time domains. Although continuous-time analysis methods are useful to explain the asymptotic dynamic behaviours of the DOB implemented by computers and microcontrollers, they fall-short in explaining the robust



a) Regulation control.



b) Trajectory tracking control.

Fig. 6. Position control responses. The parameters of the simulations are $J_m = 0.003$, $K_r = 0.25$, $K_p = 1000$, $K_D = 25$, and $T_s = 0.1$ ms.

stability and performance of the digital motion controller. For example, continuous-time analysis methods cannot explain why the digital robust motion controller becomes unstable as the phase-margin and robustness are improved by increasing α and g_{Dob} . New design constraints on the nominal plant model and the bandwidth of the DOB are analytically derived in discrete-time. One can systematically synthesise a high-performance digital robust motion controller by employing the proposed design constraints. To achieve good robust stability and performance, this paper recommends discrete-time analysis and synthesis methods for the DOB-based robust motion controllers implemented by computers.

REFERENCES

- [1] E. Sariyildiz, R. Oboe, K. Ohnishi "Disturbance Observer-based Robust Control and Its Applications: 35th Anniversary Overview," *IEEE Trans. on Ind. Electronics*, Mar. 2020, vol. 67, no. 3, pp. 2042-2053.
- [2] M. Athans, "On the LQG Problem," *IEEE Trans Automat Contr*, vol. 16, no. 6, pp. 528-528, Dec 1971.
- [3] H. Rosenbrock and P. McMorran, "Good, bad, or optimal?," *IEEE Trans Automat Contr*, vol. 16, no. 6, pp. 552-554, Dec 1971.
- [4] G. Zames, "Feedback and optimal sensitivity: Model reference transformations, multiplicative seminorms, and approximate inverses," *IEEE Trans Automat Contr*, vol. 26, no. 2, pp. 301-320, April 1981.
- [5] E. Sariyildiz, R. Mutlu, H. Yu "A Sliding Mode Force and Position Controller Synthesis for Series Elastic Actuators," *Robotica*, Jan. 2020, vol. 38, no. 1, pp. 15-28.
- [6] V. Utkin, "Variable structure systems with sliding modes," *IEEE Trans Automat Contr*, vol. 22, no. 2, pp. 212-222, Apr 1977.
- [7] J. C. Doyle, "Structured uncertainty in control system design," *IEEE Conference on Decision and Control*, Fort Lauderdale, FL, USA, 1985, pp. 260-265.
- [8] B. A. F Francis, W. M. Wonham, "The internal model principle for linear multivariable regulators," *Applied Mathematics and Optimization*, vol. 2, no. 2, pp. 170-194, June 1974.
- [9] V. L. Kharitonov, "Asymptotic stability of an equilibrium position of a family of systems of linear differential equations," *Differentsial'nye Uravnenia*, vol. 14, pp. 2086-2088, 1978.

- [10] K. Ohnishi, M. Shibata and T. Murakami, "Motion Control for Advanced Mechatronics," *IEEE/ASME Trans. Mechatron.*, vol. 1, no. 1, pp. 56-67, 1996.
- [11] F. Bechet, K. Ogawa, E. Sariyildiz, K. Ohnishi, "Electro-Hydraulic Transmission System for Minimally Invasive Robotics", *IEEE Trans. on Ind. Electronics*, Dec. 2015, vol. 62, no. 12, pp. 7643-7654.
- [12] E. Sariyildiz, C. Gong, H. Yu, "Robust Trajectory Tracking Control of Multi-mass Resonant Systems in State-Space", *IEEE Trans. on Ind. Electronics*, Dec. 2017, vol. 64, no. 12, pp. 9366 - 9377.
- [13] M. T. White, M. Tomizuka and C. Smith, "Improved track following in magnetic disk drives using a disturbance observer," *IEEE/ASME Trans Mechatron.*, vol. 5, no. 1, pp. 3-11, Mar 2000.
- [14] Z. Liu, J. Liu, L. Wang, "Disturbance observer based attitude control for flexible spacecraft with input magnitude and rate constraints," *Aerospace Science and Technology*, vol. 72, pp. 486-492, 2018.
- [15] H. Fujimoto, T. Saito, and T. Noguchi, "Motion stabilization control of electric vehicle under snowy conditions based on yaw-moment observer," in *Proc. 8th IEEE Int. Workshop Adv. Motion Control*, Kawasaki, Japan, 2004, pp. 35-40.
- [16] E. Sariyildiz, H. Sekiguchi, T. Nozaki, B. Ugurlu and K. Ohnishi, "A Stability Analysis for the Acceleration-based Robust Position Control of Robot Manipulators via Disturbance Observer," *IEEE/ASME Trans. on Mechatronics*, vol. 23, no. 5, pp. 2369-2378, Oct. 2018.
- [17] E. Sariyildiz, K. Ohnishi, "Stability and Robustness of Disturbance Observer Based Motion Control Systems", *IEEE Trans. on Ind. Electronics*, Jan. 2015, vol. 62, no. 1, pp. 414-422.
- [18] E. Sariyildiz and K. Ohnishi, "A Guide to Design Disturbance Observer," *ASME. J. Dyn. Sys., Meas., Control*, vol. 136, no. 2, pp. 1-10 (021011) Mar. 2014.
- [19] R. Bickel and M. Tomizuka, "Passivity-based versus disturbance observer-based robot control: Equivalence and stability," *ASME. J. Dyn. Sys., Meas., Control*, vol. 121, no.1, pp. 41-47, 1999.
- [20] Wen-Hua Chen, "Disturbance observer-based control for nonlinear systems," *IEEE/ASME Trans Mechatron*, vol. 9, no. 4, pp. 706-710, Dec 2004.
- [21] E. Sariyildiz, K. Ohnishi, "Analysis the robustness of control systems based on disturbance observer," *International Journal of Control*, 86:10, 1733-1743, 2013.
- [22] I. Godler, H. Honda and K. Ohnishi, "Design guidelines for disturbance observer's filter in discrete time," *International Workshop on Advanced Motion Control. Proceedings*, Maribor, Slovenia, 2002, pp. 390-395.
- [23] M. Bertoluzzo, G. S. Buja and E. Stampacchia, "Performance analysis of a high-bandwidth torque disturbance compensator," *IEEE/ASME Trans. on Mechatron.*, vol. 9, no. 4, pp. 653-660, Dec. 2004.
- [24] E. Sariyildiz, S. Hangai, T. Uzunovic, T. Nozaki, K. Ohnishi, "Stability and Robustness of the Disturbance Observer Based Motion Control Systems in Discrete-Time Domain," *IEEE/ASME Trans. Mechatron.*, DOI: 10.1109/TMECH.2020.3032115
- [25] B. Wu and E. A. Jonckheere, "A simplified approach to Bode's theorem for continuous-time and discrete-time systems," *IEEE Trans Automat Contr*, vol. 37, no. 11, pp. 1797-1802, Nov. 1992.
- [26] H S. Lee and M. Tomizuka, "Robust motion controller design for high-accuracy positioning systems," *IEEE Trans Ind. Electron*, vol. 43, no. 1, pp. 48-55, Feb. 1996.
- [27] S. Endo, H. Kobayashi, C. Kempf, S. Kobayashi, M. Tomizuka, Y. Hori, "Robust digital tracking controller design for high-speed positioning systems," *Cont Eng. Prac*, vol. 4, no 4, pp. 527 - 536, 1996.
- [28] A. Tesfaye, H. S. Lee and M. Tomizuka, "A sensitivity optimization approach to design of a disturbance observer in digital motion control systems," *IEEE/ASME Trans. Mechatron*, vol. 5, no. 1, pp. 32-38, 2000.
- [29] H. Fujimoto, Y. Hori, "High-performance servo systems based on multirate sampling control," *Cont Eng Prac*, vol.10, pp.773-781, 2002.
- [30] X. Chen and M. Tomizuka, "Optimal plant shaping for high bandwidth disturbance rejection in discrete disturbance observers," *Proceedings of the 2010 American Control Conference*, Baltimore, MD, 2010, pp. 2641-2646.
- [31] K. Kong and M. Tomizuka, "Nominal model manipulation for enhancement of stability robustness for disturbance observer-based control systems," *International Journal of Control, Automation, and Systems*, vol. 11, no. 1, pp. 12-20, Feb. 2013.
- [32] R. Antonello, K. Ito, R. Oboe, "Acceleration Measurement Drift Rejection in Motion Control Systems by Augmented-State Kinematic Kalman Filter," *IEEE Trans. Ind. Electron.*, vol. 63, no. 3, pp. 1953-1961, Mar. 2016.
- [33] T. Uzunovic, E. Sariyildiz and A. Sabanovic, "A discussion on discrete implementation of disturbance-observer-based control," *International Workshop on Advanced Motion Control*, Tokyo, 2018, pp. 613-618.
- [34] E. Sariyildiz, R. Mutlu, C. Zhang, "Active Disturbance Rejection Based Robust Trajectory Tracking Controller Design in State Space," *ASME. J. Dyn. Sys., Meas., Control*, June 2019; 141(6): 061013.
- [35] E. Sariyildiz, K. Ohnishi, "Performance and robustness trade-off in disturbance observer design," *39th Annual Conference of the IEEE Industrial Electronics Society*, Vienna, 2013, pp. 3681-3686.